JOURNAL OF APPLIED ELECTROCHEMISTRY **21** (1991) 2–5

The wall-jet electrode and the study of electrode reaction mechanisms: the EC′(catalytic) mechanism

R. G. COMPTON, A. C. FISHER, G. P. TYLEY

Physical Chemistry Laboratory, Oxford University, South Parks Road, Oxford OX1 3QZ, UK

Received 13 February 1990; revised 25 March 1990

The theory of EC′(catalytic) reactions at the wall-jet electrode is developed using a computational procedure based on the Expanding Grid Backwards Implicit method. In particular, it is shown that the variation of the transport limited current with solution flow rate provides a means of characterising the EC′ mechanism. A working curve is presented which shows how the effective number of electrons transferred depends on a normalized rate constant and this permits the analysis of experimental data and the deduction of the homogeneous rate constant of the catalytic chemical reaction, for arbitrary electrode geometry, without recourse to further computation.

1. Introduction

An important general type of electrode reaction mechanism is the so-called catalytic (EC′) mechanism [1] in which an electrogenerated species (the 'mediator') oxidizes or reduces some other solution species (the 'substrate') with the regeneration of the original electroactive material which can thus undergo further electron transfer at the electrode. The process has importance both in the kinetic characterisation of reaction intermediates and for synthesis where the possibility of homogeneous catalysis of electrochemical reactions is attractive [2]. In its simplest form, the mechanism is defined by the following kinetic scheme:

$$\mathrm{A} +/- e^- \rightleftharpoons \mathrm{B} \qquad \text{(i)}$$

$$\mathrm{B} + \mathrm{Y} \xrightarrow{\tilde{k}} \mathrm{A} + \text{products} \qquad \text{(ii)}$$

In experimental practice Y is often in excess so that the chemical step obeys pseudo-first-order kinetics (rate constant $\tilde{k}$ [3].

The wall-jet electrode (WJE) is a well-defined hydrodynamic electrode in which the flow is due to a jet of liquid which strikes a planar electrode surface at right angles and spreads out radially over that surface, the fluid outside the jet being at rest [4]. The electrode is, in principle, well-suited to the study of electrode reaction mechanisms. Accordingly in a previous paper [5] we developed a general computational method for solving mass transport problems involving WJEs and, in particular, developed the theory for, firstly, the transport limited current/flow rate behaviour for simple electron transfer reactions [5], and for ECE and DISP1 processes [5, 6], and, secondly, showed how to compute current/voltage voltammetric waveshapes and thus deduced the halfwave potential/flow rate characteristics of an EC process [7]. In this paper we continue our study of the application of the WJE to electrode reaction mechanisms and develop the theory of catalytic reactions at the WJE in respect of their limiting current/flow rate diagnostics.

2. Theory

The convective-diffusion equations relevant to the EC′, mechanism in the WJE geometry, under steady-state conditions are:

$$v_r \frac{\partial[\mathrm{A}]}{\partial r} + v_z \frac{\partial[\mathrm{A}]}{\partial z} = D \frac{\partial^2[\mathrm{A}]}{\partial z^2} + \tilde{k}[\mathrm{B}][\mathrm{Y}] \qquad (1)$$

$$v_r \frac{\partial[\mathrm{B}]}{\partial r} + v_z \frac{\partial[\mathrm{B}]}{\partial z} = D \frac{\partial^2[\mathrm{B}]}{\partial z^2} - \tilde{k}[\mathrm{B}][\mathrm{Y}] \qquad (2)$$

$$v_r \frac{\partial[\mathrm{Y}]}{\partial r} + v_z \frac{\partial[\mathrm{Y}]}{\partial z} = D \frac{\partial^2[\mathrm{Y}]}{\partial z^2} - \tilde{k}[\mathrm{B}][\mathrm{Y}] \qquad (3)$$

where the cylindrical coordinates r and z represent the radial direction and distance normal to the electrode surface, respectively and D is the diffusion coefficient of A, B and Y assumed to be all equal. v_r and v_z are the components of the solution velocity in the r and z directions, respectively. Notice that in writing the mass transport equations we have neglected radial diffusion. This has been shown to be a good approximation for practical electrodes [8].

Close to the electrode surface, the following approximations have been derived [8] for the velocity components:

$$v_{r,\eta\to 0} = (2/9)(15M/2\nu r^3)^{1/2}\eta \qquad (4)$$

$$v_{z,\eta\to 0} = (7/36)(40M\nu/3r^5)^{1/4}\eta^2 \qquad (5)$$

where η is the normalized parameter describing distance perpendicular to the electrode:

$$\eta = (135M/32\nu^3 r^5)^{1/4} z, \qquad (6)$$

ν is the kinematic viscosity of the solution (cm^2 s^{-1}) and

$$M = k_c^4 V_f^3 / 2\pi^3 a^2, \qquad (7)$$

where V_f is the volume flow rate ($\mathrm{cm}^3\,\mathrm{s}^{-1}$), k_c is a constant found experimentally to be approximately 0.90 [8] and a is the jet diameter.

We assume that there are finite bulk concentrations; $[\mathrm{A}]_0$ and $[\mathrm{Y}]_0$, of A and Y are zero of B. It is helpful to normalize the concentrations: $g(\mathrm{A}) = [\mathrm{A}]/[\mathrm{A}]_0$, $g(\mathrm{B}) = [\mathrm{B}]/[\mathrm{A}]_0$ and $g(\mathrm{Y}) = [\mathrm{Y}]/[\mathrm{Y}]_0$. The boundary conditions corresponding to the transport limited reduction (oxidation) of A are:

(a) at the centre of the jet,

$$r = 0: \qquad g(\mathrm{A}) = 1, \quad g(\mathrm{B}) = 0, \quad g(\mathrm{Y}) = 1 \tag{8}$$

(b) in bulk solution,

$$z \longrightarrow \infty (\eta \sim 0.4):$$

$$g(\mathrm{A}) = 1, \quad g(\mathrm{B}) = 0, \quad g(\mathrm{Y}) = 1 \tag{9}$$

(c) at the electrode surface,

$$z = 0: \qquad g(\mathrm{A}) = 0, \quad \partial g(\mathrm{A})/\partial z = -\partial g(\mathrm{B})/\partial z, \quad \partial g(\mathrm{Y})/\partial z = 0 \tag{10}$$

Notice that we consider $\eta > 0.4$ as corresponding to bulk solution since we have shown previously that this is the region in which only negligible deviations from bulk concentrations are found [5].

In order to solve the above equations and boundary conditions we use the 'expanding grid' Backwards Implicit Finite Difference (BIFD) method [5]. In the following we adopt exactly the same approch and notation used in [5] which should be consulted for full computational and methodological detail. In particular we use subscripts on the normalized concentration $g_{j,k+1}$ to denote distances in the radial ($j = 1, 2, \ldots J$) and normal ($k = 1, 2, \ldots K$) directions. A normalized concentration with a primed subscript, $g_{j,k'}$, represents an interpolated concentration (deduced from $g_{j,k}$) which is used in the calculation of $g_{j,k+1}$ [5].

Thus, following [5] we arrive at three matrix equations, one for each of i = A, B and Y, such that,

$$\{\mathbf{d}\}^i = [\mathbf{T}]^i \cdot \{\mathbf{u}\}^i \tag{9}$$

The matrix elements in each case are readily deduced to be: (a) i = A

$$d_j = g(\mathrm{A})_{j,k'} + K_{j,k+1} \cdot g(\mathrm{B})_{j,k+1} \cdot g(\mathrm{Y})_{j,k+1} \qquad j = 1, 2, \ldots \overline{J-2} \tag{10}$$

$$D_{J-1} = g(\mathrm{A})_{J-1,k'} + K_{J-1,k+1} \cdot g(\mathrm{B})_{J-1,k+1} \cdot g(\mathrm{Y})_{J-1,k+1} + \{\varepsilon_{J-1,k+1} - \lambda_{J-1,k+1}\} \tag{11}$$

$$u_j = g(\mathrm{A})_{j,k+1} \qquad j = 1, 2, \ldots \overline{J-1} \tag{12}$$

$$a_j = -\varepsilon_{j,k+1} \qquad j = 2, 3 \ldots \overline{J-1} \tag{13}$$

$$b_j = (2\varepsilon_{j,k+1} - \lambda_{j,k+1} + 1) \qquad j = 1, 2 \ldots \overline{J-1} \tag{14}$$

$$c_j = [\lambda_{j,k+1} - \varepsilon_{j,k+1}] \qquad j = 1, 2 \ldots \overline{J-2} \tag{15}$$

(b) i = B

$$d_j = g(\mathrm{B})_{j,k'} - K_{j,k+1} \cdot g(\mathrm{B})_{j,k+1} \cdot g(\mathrm{Y})_{j,k+1} \qquad j = 2, 3 \ldots \overline{J-1} \tag{16}$$

$$d_1 = g(\mathrm{B})_{1,k'} - K_{1,k+1} \cdot g(\mathrm{B})_{1,k+1} \cdot g(\mathrm{Y})_{1,k+1} + \varepsilon_{1,k+1} \tag{17}$$

$$u_j = g(\mathrm{B})_{j,k+1} \qquad j = 1, 2 \ldots \overline{J-1} \tag{18}$$

$$a_j = -\varepsilon_{j,k+1} \qquad j = 2, 3 \ldots \overline{J-1} \tag{19}$$

$$b_j = (2\lambda_{j,k+1} - \varepsilon_{j,k+1} + 1) \qquad j = 1, 2 \ldots \overline{J-1} \tag{20}$$

$$c_j = [\lambda_{j,k+1} - \varepsilon_{j,k+1}] \qquad j = 1, 2 \ldots \overline{J-2} \tag{21}$$

(c) i = Y

$$d_j = g(\mathrm{Y})_{j,k'} - \{[\mathrm{A}]_0/[\mathrm{Y}]_0\} K_{j,k+1} \cdot g(\mathrm{B})_{j,k+1} \cdot g(\mathrm{Y})_{j,k+1} \qquad j = 1, 2 \ldots \overline{J-2} \tag{22}$$

$$d_{J-1} = g(\mathrm{Y})_{J-1,k'} - \{[\mathrm{A}]_0/[\mathrm{Y}]_0\} K_{J-1,k+1} \cdot g(\mathrm{B})_{J-1,k+1} \cdot g(\mathrm{Y})_{J-1,k+1} - \{[\mathrm{Y}]_0/[\mathrm{A}]_0\}[\lambda_{J-1,k+1} - \varepsilon_{J-1,k+1}] \tag{23}$$

$$u_j = g(\mathrm{Y})_{j,k+1} \qquad j = 1, 2 \ldots \overline{J-1} \tag{24}$$

$$a_j = -\varepsilon_{j,k+1} \qquad j = 2, 3 \ldots \overline{J-1} \tag{25}$$

$$b_j = (2\varepsilon_{j,k+1} - \lambda_{j,k+1} + 1) \qquad j = 2, 3 \ldots \overline{J-1} \tag{26}$$

$$b_1 = (\varepsilon_{1,k+1} - \lambda_{1,k+1} + 1) \tag{27}$$

$$c_j = [\lambda_{j,k+1} - \varepsilon_{j,k+1}] \qquad j = 1, 2 \ldots \overline{J-2} \tag{28}$$

where $\varepsilon_{j,k+1}$ and $\lambda_{j,k+1}$ have been defined in reference [13] and

$$K_{j,k+1} = \frac{[\mathrm{Y}]_0 \tilde{k} \Delta r}{v_r(j, k+1)}, \tag{29}$$

in which Δr is the size of the simulation grid in the radial direction.

The matrix Equations 9 may be readily solved for a chosen electrode geometry and rate constant, $\tilde{k}$, as described previously [5] but note that since the matrix elements for A depend on $g(\mathrm{B})_{j,k+1}$ and $g(\mathrm{Y})_{j,k+1}$ and those for B and Y are also interrelated we have to adopt an iterative procedure as with the calculations on the DISPI mechanism [5]. Having calculated the concentration profiles $g(i)_{j,k}$ for i = A, B, Y, $0 < j < J$ and $0 < k < K$ the current at the electrode may be found using Equation 41 in [5].

Computations were carried out using programs written in FORTRAN 77 on a VAX 11/785 mainframe computer, using NAG 11 library routines.

3. Results and discussion

Calculations were carried out as outlined above for parameters in the following ranges: electrode radius, $R = 0.40$–$1.0\,\mathrm{cm}$; $a = 0.0345\,\mathrm{cm}$, $V_\mathrm{f} = 10^{-4}$ to $10^{-1}\,\mathrm{cm^3\,s^{-1}}$; $D = 2 \times 10^{-6}$ to $2 \times 10^{-3}\,\mathrm{cm^2\,s^{-1}}$; and $\tilde{k} = 0$–$10^2\,\mathrm{mol^{-1}\,dm^3\,s^{-1}}$ for $\nu = 0.0089\,\mathrm{cm^2\,s^{-1}}$ (H_2O) and $[\mathrm{A}]_0 = 10^{-6}\,\mathrm{mol\,cm^{-3}}$. In the cases when $\tilde{k} = 0$ the computed transport limited currents were in agreement with the analytical equation derived by Albery [8] for the no-kinetics case:

$$I_\mathrm{LIM} = 1.59 k_\mathrm{c} F D^{2/3} \nu^{-5/12} V_\mathrm{f}^{3/4} a^{-1/2} R^{3/4} [\mathrm{A}]_0 \quad (30)$$

where F is the Faraday constant. In all calculations convergence was examined by varying the size of the computational grid used: for $\tilde{k} = 0$ values of $J = 200$ and $K = 5000$ were sufficient to give convergence to three significant figures in the computed current. These values increase with $\tilde{k}$: for $\tilde{k} = 10$ values of $J = 600$ and $K = 6000$ were needed. This is because the perturbations of the B and Y concentration profiles from their bulk values are increasingly constrained to within smaller distances of the electrode due to their more rapid reaction.

Figure 1 shows how the transport limited current varies with flow rate for an electrode of geometry defined by $R = 0.4\,\mathrm{cm}$, $a = 0.0345\,\mathrm{cm}$ and a species such that $D = 2 \times 10^{-6}\,\mathrm{cm^2\,s^{-1}}$ and $[\mathrm{A}]_0 = 10^{-6}\,\mathrm{mol\,cm^{-3}}$. It is assumed that $[\mathrm{Y}]_0 \gg [\mathrm{A}]_0$ and that $\tilde{k}[\mathrm{Y}]_0 = 10\,\mathrm{s^{-1}}$. Also shown in the behaviour predicted by Equation 30 for a kinetically uncomplicated reaction with the same parameters. Notice that at high flow rates the behaviour of the simple E reaction and the EC′ process are indistinguishable since B is swept away from the electrode surface before reaction (ii) can regenerate A, but that at low flow rates extra current flows due to the catalytic process. The form of this curve is characteristic of an EC′ reaction.

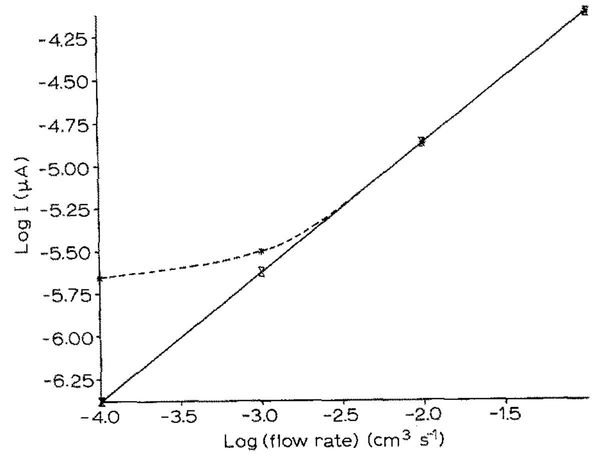

Fig. 1. The variation of the transport limited current with flow rate for (a) a simple electron transfer reaction (——), and (b) an EC′ (catalytic) reaction (- - -), with the parameters specified in the text. Notice that both scales are logarithmic and that in the former case the straight line has the slope of 3/4 required by Equation 30.

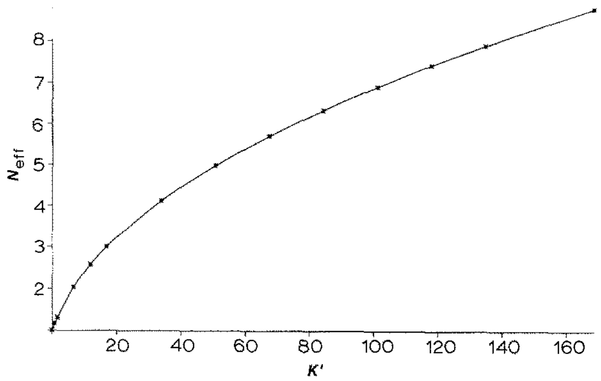

Fig. 2. A working curve for the case of pseudo-first-order kinetics ($[\mathrm{Y}]_0 \gg [\mathrm{A}]_0$) relating the effective number of electrons transferred, N_eff, to the normalized rate constant, K', defined in Equation 31.

The theory presented above allows the calculation of the transport limited current for chosen rate constants and electrode geometrics. However, a modification of an argument presented for the case of EC reactions at a WJE [7] suggests that for a given value of $[\mathrm{Y}]_0/[\mathrm{A}]_0$ the 'effective' number of electrons transferred, N_eff (i.e. the ratio of the current flowing in an EC′ reaction to that which would flow under corresponding conditions for a simple electron transfer reaction), is a unique function of the following dimensionless rate constant,

$$K' = \tilde{k}[\mathrm{Y}]_0 R^{5/2} (64/81 C^2 D)^{1/3} \quad (31)$$

where $C = ([5M]^3/216\nu^5)^{1/4}$. Computations showed that for fixed $[\mathrm{Y}]_0/[\mathrm{A}]_0$, N_eff was indeed a unique function of K', and this allowed the deduction of 'working curves' for different $[\mathrm{Y}]_0/[\mathrm{A}]_0$ showing the variation of N_eff with K'. As alluded to in the introduction the most usual experimental situation corresponding to pseudo-first-order kinetics, i.e. $[\mathrm{Y}]_0 \gg [\mathrm{A}]_0$. Hence Fig. 2 shows the working curve relating to this case. This provides the basis for the analysis of experimental data: observed values of N_eff are related to corresponding K' values which should then have a flow rate dependence in agreement with Equation 31. The parameter K' also controls the point at which the current/flow rate plot in Fig. 1 deviates from linearity: clearly larger rate constants are required to achieve this in systems of greater diffusion coefficient.

In conclusion we have demonstrated that the 'expanding grid' BIFD method can be used to calculate the transport limited current/flow rate behaviour for an EC′ reaction. The results give rise to 'universal' working curves for different values of the ratio $[\mathrm{Y}]_0/[\mathrm{A}]_0$, which provide a means for the characterization of the reaction type and for the deduction of the rate constant $\tilde{k}$.

References

[1] C. P. Andrieux and J. M. Saveant, 'Investigations of Rates

and Mechanisms of Reactions, Part 2, in 'Techniques of Chemistry', Vol. 6 (edited by C. F. Bernasconi), John Wiley, New York (1986) p. 305–90.

[2] H. Lund, *J. Mol. Catal.* **38** (1986) 203.

[3] A. J. Bard and L. R. Faulkner, 'Electorchemical Methods', John Wiley, New York (1980).

[4] M. B. Glauert, *J. Fluid Mech.* **1** (1956) 625.

[5] R. G. Compton, C. R. Greaves and A. M. Waller, *J. Appl. Electrochem.*, in press.

[6] *Idem*, *ibid.*, in press.

[7] R. G. Compton, A. C. Fisher and G. P. Tyley, *ibid.*, submitted for publication.

[8] W. J. Albery and C. M. A. Brett, *J. Electroanal. Chem.* **148** (1983) 211.